Simulating wetting front dimensions of drip irrigation systems: Multi criteria assessment of soft computing models

Article *in* Journal of Hydrology · March 2020

DOI: 10.1016/j.jhydrol.2020.124792

CITATIONS
11

READS
130

5 authors, including:

Jalal Shiri
University of Tabriz
146 PUBLICATIONS **4,741** CITATIONS
SEE PROFILE

Bakhtiar Karimi
University of Kurdistan
35 PUBLICATIONS **104** CITATIONS
SEE PROFILE

Mohammad Hossein Kazemi
University of Tabriz
6 PUBLICATIONS **36** CITATIONS
SEE PROFILE

Sepideh Karimi
University of Tabriz
27 PUBLICATIONS **547** CITATIONS
SEE PROFILE

Journal of Hydrology 585 (2020) 124792

Contents lists available at ScienceDirect

Journal of Hydrology

journal homepage: www.elsevier.com/locate/jhydrol

Research papers

Simulating wetting front dimensions of drip irrigation systems: Multi criteria assessment of soft computing models

Jalal Shiri[a,b], Bakhtiar Karimi[c,*], Nazir Karimi[c], Mohammad Hossein Kazemi[a], Sepideh Karimi[a]

[a] Water Engineering Department, Faculty of Agriculture, University of Tabriz, Tabriz, Iran
[b] Center of Excellence in Hydroinformatics, Faculty of Civil Engineering, University of Tabriz, Iran
[c] Department of Water Science and Engineering, University of Kurdistan, Sanandaj, Iran

ARTICLE INFO

This manuscript was handled by G. Syme, Editor-in-Chief

Keywords:
Artificial intelligence
Irrigation systems
k-Fold testing
Wetting bulb

ABSTRACT

Accurate estimation of wetting front dimensions in surface and sub-surface irrigation systems is very important for optimal management of water resources as well as increasing the performance of irrigation systems. Analytical and numerical models need lots of computational efforts and costs, so their applications in practical issues might be difficult. Meanwhile, artificial intelligence models could be suitable substitutes for these models. The present study aimed at simulating wetting front (wetting bulb) dimensions in different soil types for surface and sub-surface irrigation systems using continuous and pulse applications, through the gene expressions programming (GEP) and random forest (RF) techniques. Different experiments were carried out to achieve the required data. A robust k-fold testing data scanning technique was adopted for assessing the applied models, where different criteria were considered for defining the "k" values per test procedure. The results obtained revealed that, with minor exceptions, both the applied GEP and RF models presented good ability in modeling the wetting front dimensions in all the conducted treatments. The results also showed that soil type and emitter installation depth were the best criteria for defining the "k" values of k-fold testing procedure for the surface and sub-surface irrigation systems, respectively.

1. Introduction

Drip irrigation systems have been widely developed worldwide during the recent decades. When designed good and operated suitably, these systems help to achieve maximum crop yield. Drip irrigation systems reduce water applications and can be useful tools for increasing water use efficiency and productivity (Al-Ogaidi et al., 2016; Khanmohammadi and Besharat, 2018). However, when poorly designed and/or operated incorrectly, the actual performance of drip systems can be much lower than their potential capability (Al-Ogaidi et al., 2016). On the other hand, suitable design and management of these systems requires understanding of the precise distribution of wetting pattern around the emitters (Kandelous et al., 2011). During the past decades, substantial studies have been performed to determine the wetting patterns of the point and line sources. The diameter and depth of wetting pattern are the basic parameters of moisture front distribution (Liu and Xu, 2018; Khattak et al., 2017). The depth of the wetting front ought to be identified with expected root zone depth, while its diameter is dependent to the spaces between the emitters and laterals. The main parameters of the wetted zone are shown in Fig. 1 for surface and subsurface drip irrigation systems. So far, different methods have been developed for estimating the dimensions of the soil wetted pattern under drip irrigation systems. The most common models are the empirical, analytical and numerical models (Subbaiah, 2013). Empirical models (Schwartzman and Zur, 1986; Singh et al., 2006; Amin and Ekhmaj, 2006; Kandelous et al., 2008; Malek and Peters, 2011; Al-Ogaidi et al., 2016) have been developed using a regression analysis of field/laboratory-based data. Further, analytical (Hammami and Zayani, 2016; Cook et al., 2003) and numerical (Šejna et al., 2014; Elmaloglou et al., 2013; Arbat et al., 2013) models solve the governing flow equations (e.g. Richards equation) under particular initial and boundary conditions. Analytical and numerical models require significant computing time and high skills to be applied; so it is difficult to employ them for design purposes. Also, empirical models, despite their simplicity, are site specific and cannot be generalized. Hence, it is necessary to apply a suitable technique to estimate the wetting pattern dimensions with an acceptable accuracy and lower computational costs for wide range of influential factors, e.g. emitter discharge, emitter installation depth, elapsed time, saturated hydraulic conductivity, soil bulk density, initial moisture content and soil texture.

* Corresponding author.
E-mail address: Bakhtiar.karimi@uok.ac.ir (B. Karimi).

https://doi.org/10.1016/j.jhydrol.2020.124792
Received 15 December 2019; Received in revised form 29 January 2020; Accepted 1 March 2020
Available online 04 March 2020

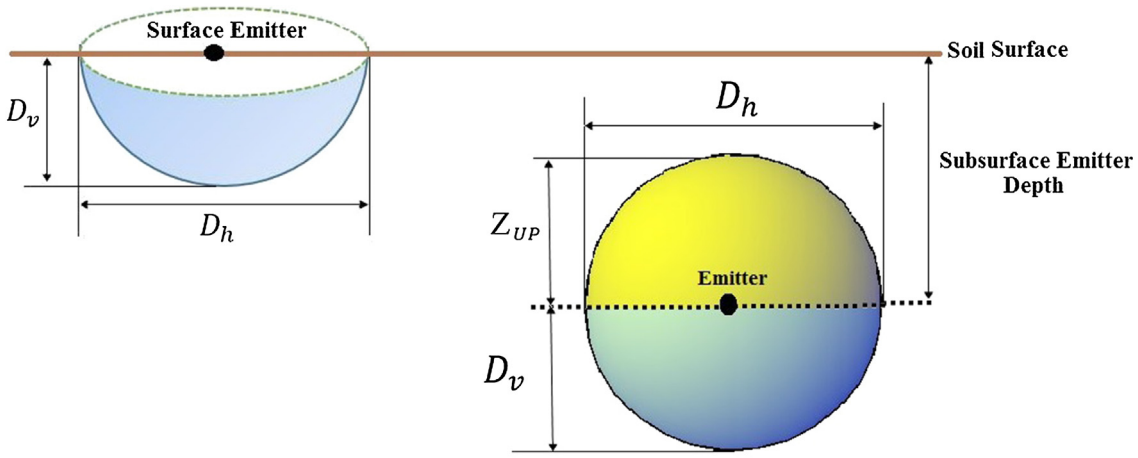

Fig. 1. Schematic representation of the wetting pattern under surface and subsurface drip irrigation (D_h: wetting diameter, D_V: wetting depth, Z_{up}: upward water movement in subsurface irrigation system).

Consequently, soft computing techniques can be suitable alternatives to simulate wetting front dimensions. These models can be categorized as empirical regression-based models, where the relations between independent and dependent variables are discovered and studied. Soft computing-based techniques [e.g. gene expression programming (GEP) and random forest (RF)] have been applied in different water resources engineering disciplines due to strong recognition pattern which can relate the inputs to the target parameter(s) (Maroufpoor et al., 2019).

Applications of these approaches in different fields of water resources engineering have been reported in this context, including e.g. modeling water distribution uniformity in sprinkler irrigation (Maroufpoor et al., 2019), simulating water front advance of furrow irrigation (Golestani Kermani et al., 2019), modeling wind drift and evaporation losses from sprinkler irrigation (Maroufpoor et al., 2018; Al-Ghobari et al., 2018), estimating crop water requirement (Landeras et al., 2018), estimation of dew point temperature, soil water capacity and bulk density (Shiri et al., 2014, 2017a,b, respectively) and modeling friction factor in irrigation pipes (Najafzadeh et al., 2018).

Meanwhile, most of the investigations aimed to estimate the wetting pattern dimensions for surface drip irrigation systems with continuous (Singh et al., 2006; Karimi and Mohammadi, 2018; Ekhmaj et al., 2007; Kandelous et al., 2008; Lazarovitch et al., 2009; Kandelous and Simunek, 2010a; Hinnell et al., 2010; Karimi et al., 2015) and pulse (Karmeli and Peri, 1974; Mostaghimi and Mitchell, 1983; Elmaloglou and Diamantopoulos, 2009; Mohammadbeigi et al., 2017) application modes. Nonetheless, most of the studies have used a single data assigning procedure (2-block data partitioning) where a certain block of available patterns (data) are used for training the models and then, the developed/trained models are tested using an independent data set, which might be misleading. Nevertheless, application of GEP and RF in such kinds of studies is rare in literature. So, there is a room to extend such kind of investigations for modeling wetting dimensions of surface/subsurface irrigation systems with either continuous and pulse application modes. The present study aimed at simulating horizontal and vertical wetting dimensions of the surface and subsurface drip irrigation systems with continuous and pulse application modes using the GEP and RF techniques assessed by the robust k-fold testing data scanning procedure.

2. Material and methods

2.1. Laboratory experiments and used data

The laboratory experiments were carried out at the central laboratory of the Agricultural College of University of Kurdistan, Iran. A soil container with a length of 3 m, width of 0.5 m, and height of 1 m was used in the experiments. One side of this container is plexiglass sheets to monitor the advance of wetting patterns at different times during the experiments. Three air-dried soil samples were filled into the lysimeter according to bulk density of each soil. Table1 presents the physical properties of the studied soil samples. Fig. 2 shows the studied soils' texture graph. For soil stability and uniform initial water distribution, the soil container was left in the laboratory form 24 to 48 h. Moreover, to prevent preferential flow along the walls, lysimeter walls were treated with glue and sprayed with sand to create a coarse surface (Kandelous and Simunek, 2010b). The reservoir volume was 200 L, containing a float to keep a constant water level. A pressure gauge and a ball valve were placed in discharge pipe of the pump for measuring the system pressure and maintaining the steady discharge. All the experiments were performed at a fixed pressure (i.e. 2 bars). Emitter clogging based suspended particle was prevented by the filtration system. An off–on valve placed between the lateral and sub-main to control flow inside each container. Moreover, to achieve high uniformity in subsurface irrigation system, emitters were placed on soil surface (in the middle of one of the lysimeter walls) and water flow was delivered to certain depths through a thin tube with a diameter of 5 mm, as advised by Kandelous and Simunek (2010b). Emitters were connected to a water reservoir by micro polyethylene tubes (main, sub-main and lateral tubes with diameters of 32, 20 and 16 mm, respectively). Considering low discharge rate in each experiment, a by-pass assembly was installed to regulate inflow and return additional water to reservoir. The wetting front and water distribution were evaluated in light, medium and heavy-textured homogeneous soils. The length of the containers for all the soil textures was 1 m. Fig. 3 shows the schematic description of experimental device. This container represents half space of the complete cylinder i.e. half of the wetted zone, so, the actual emitter discharges were multiplied by 2 (Kandelous and Simunek, 2010a, Al-Ogaidi et al., 2016). The saturated hydraulic conductivity was estimated using Rosetta software (Schaap et al., 2001). A total of 108 experiments (36 and 72 experiment for surface and subsurface drip irrigation systems, respectively) were conducted with three discharge rates of 2, 4 and 6 L/h. The experiments were carried out for two continuous and pulse application modes. In pulse application, the pulse cycles were considered as 30–30, 20–40 and 40–20 min (The first shows the irrigation time (on) and the second denotes the rest time (off) of the system). The irrigation time was set as 4 h and emitters were placed at three depths of 0, 15 and 30 cm below the soil surface. The locations of the wetting patterns were recorded by drawing them on the plexiglass walls at specified times. At the end of each experiment, graded tapes in

Table 1
Overview of the used independent variables.

General soil information

Samples	Soil texture	Sand (%)	Silt (%)	Clay (%)	Bulk density (gr/cm^3)	Saturated hydraulic conductivity (cm/h)
Heavy texture	Clay	26	26	48	1.3	0.85
Medium texture	Sandy-clay-loam	50	18	32	1.36	0.92
Light texture	Loam-sandy	82	6	12	1.53	3.95

Statistical parameters of the applied input variables

	max	min	mean	SD	CV
Q	12	4	7.79	3.26	0.42
Ks	3.95	0.85	1.78	1.4	0.78
Sand	82	26	50.52	22.67	0.45
Silt	26	6	17.43	8.11	0.46
Clay	48	12	32.04	14.57	0.45
ρ_b	1.53	1.3	1.39	0.1	0.07
θ_0	4.16	1.3	2.58	0.78	0.3
Emitter depth	30	15	22.55	7.5	0.33
Tirr/Tt	0.67	0.33	0.48	0.14	0.3

Note: Q = discharge (lit/h), K_S = saturated hydraulic conductivity (cm/hr), ρ_b = soil bulk density (gr/cm^3), θ_0 = soil initial moisture content, Tirr/Tt = the ratio of irrigation cycle time to the total time of the irrigation process (in pulse irrigation applications), SD = standard deviation, CV = coefficient of variation.

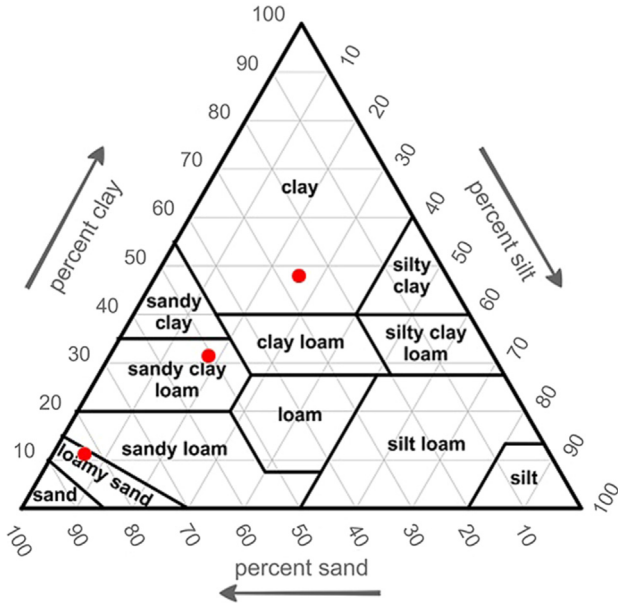

Fig. 2. Texture graph of the studied soil samples.

lysimeter body were used for preparing the shape of wetting zone. The coordinates of the horizontal and vertical wetting patterns were digitized using Grapher software version 7. Finally, the values of wetted dimensions in horizontal and vertical directions were calculated.

2.2. Gene expression programming (GEP)

Alike to genetic programming (GP), GEP imitates the biological evolution for making a computer program that can simulate the target parameter. The problems are encoded in fixed-length linear chromosomes (Ferreira, 2006). A strong aspect of GEP is its capability in presenting the models' mathematical expressions that have related the input-target parameters, which can be transferable to other patterns.

By using the GEP method, the first step is selecting the proper fitness function. The root relative squared error (RRSE) was used as the fitness function according to literature for the same kinds of studies (Maroufpoor et al., 2019). The second step consists of defining the terminal (input-target pairs) and functions sets. Terminal set includes the independent (input) variables (see Section 2.5) as well as the simulated targets (wetting front dimensions in all treatments). According to Koza (1994), the first functions that should be used in simulation issues are the four basic mathematical operators (+,-,/,*). Here, a set of mathematical functions consisted of the main functions {+, −, ×, ÷}, trigonometric functions, and other mathematical functions {√, x2, exp}, as advised in such kinds of studies. The third step with GEP establishment is defining the architecture of GEP chromosomes that were selected as length of head = 8 and gene numbers per chromosome = 3 according to Ferreira (2001). The next step is defining the linking function, with which, the sub-trees of GEP are linked together. Among four possibilities for this function (addition, multiplication, subtraction and division), addition linking function was selected as this is the commonly used function in simulation issues as advised by Ferreira (2006). The last phase of GEP implementation is selecting the basic genetic operators (mutation rate, etc) that were used as default values of GeneXpro program. Fig. 4 shows a schematic GEP representation, where GEP flowchart is completed each time to obtain the GEP-based model that relates the input variables to targets.

2.3. Random forest (RF)

Random Forests (RF), a group learning algorithm, handles high-dimension regressive issues. As a tree-based group method, all trees in RF are dependent of a series of random variables, and the forest is grown from many regression trees put together and form a group (Breiman, 2001). The final decision is a consequence of averaging the output following the fitting individual trees in ensemble (bagging procedure). The bias of the bagged trees is the same of the single trees, whereas the variance is decreased by reducing the correlation between the trees (Hastie et al., 2009).

RFs for regression are formed by growing trees depending on a random vector, Θ so that tree predictor $h(X, \Theta)$ can take on numerical magnitudes. The mean-squared generalization error of each numerical estimator $h(X)$ is (Breiman, 2001):

$$E_{X,Y}(Y - h(X))^2 \quad (1)$$

RF estimator is formed through making an average over the j^{th} tree. In this case, the following two basic theorems stand:

Theorem1. By increasing the number of trees in the forest:

$$E_{X,Y}(Yav_j h(X, \Theta_j))^2 \rightarrow E_{X,Y}(Y - E_\Theta h(X, \Theta))^2 \quad (2)$$

The right hand of the above equation illustrates the generalization

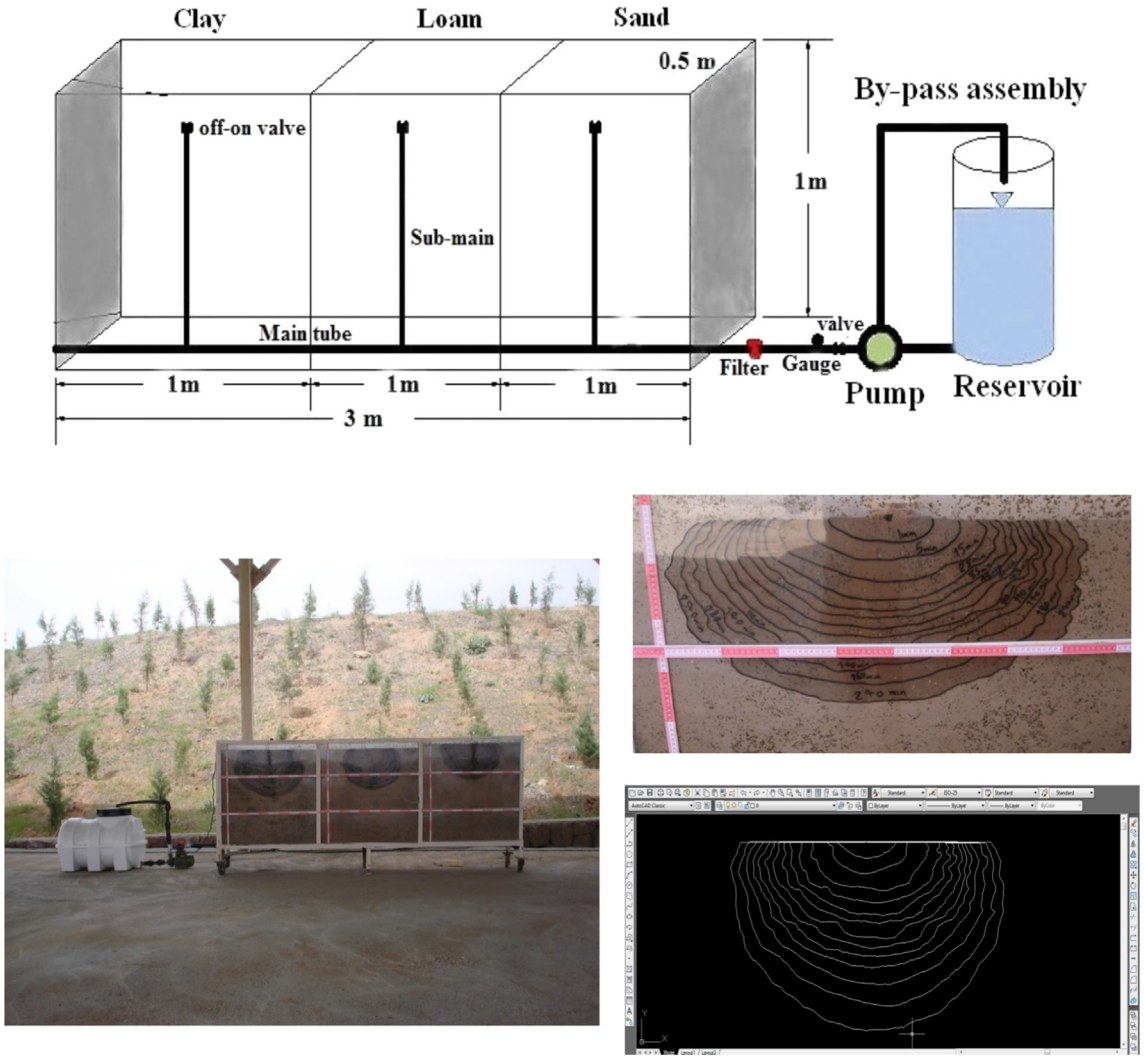

Fig. 3. Schematic view of the experimental device.

error of the forest. Similarly, the average generalization error of a tree is (Breiman, 2001):

$$PE*(tree) = E_{\Theta}E_{X,Y}(Y - h(X,\Theta))^2 \quad (3)$$

Theorem2. Suppose that $EY = E_X h(X,\Theta)$ for all Θ, so:

$$PE*(forest) \leqslant \bar{\rho}.\ PE*(tree) \quad (4)$$

In which, $\bar{\rho}$ denotes the weighted correlation between the residuals $Y - h(X,\Theta)$ and.$Y - h(X,\Theta')$ Θ and Θ' are independent variables (Breiman, 2001). Fig. 5 shows a general view of the RF method. Various numbers of RF trees were examined here to find the optimum tree number. Optimum tree numbers were different for each analyzed case and more detailed information in this regard will be given in the next sections. Further, 10 cycles were found as the best cycle number for calculating the mean error. The percentage decrease in training error was found as 5%, iteratively. Minimum child node size to stop and the maximum number of levels were selected as 5, and 10, respectively (based on trial and error process).

2.4. Commonly used empirical models

In order to assess the performance of the developed soft computing approaches with respected to the traditional methods, two commonly used models were applied and compared with GEP and RF. Schwartzman and Zur (1986) introduced an empirical model for simulating wetting front dimensions under surface drip irrigation systems. Their model stands on relating the emitter discharge Q (m3 s-1), saturated hydraulic conductivity Ks (m s^{-1}) and total volume of applied water $V_w(m^3)$, to the diameter and depth of water front, as follows:

$$D_h = 1.82(V_w)^{0.22}\left(\frac{K_s}{Q}\right)^{-0.17} \quad (5)$$

$$D_V = 2.54(V_w)^{0.63}\left(\frac{K_s}{Q}\right)^{0.45} \quad (6)$$

Kandelous et al. (2008) developed empirical equations for estimating wetting front dimension from the subsurface continuous irrigation systems as:

$$D_{h=} = 4.244V_W^{0.526}\left(\frac{K_s}{Q}\right)^{0.026} \quad (7)$$

$$D_V = 0.66V_W^{0.333}\left(\frac{K_s}{Q}\right)^{-0.167} \quad (8)$$

$$Z_{up} = 0.72V_W^{0.344}\left(\frac{K_s}{Q}\right)^{-0.156} \quad (9)$$

To the best of the authors' knowledge, there is no recommended model for estimating wetting dimensions of pulse irrigation systems among the traditional methods.

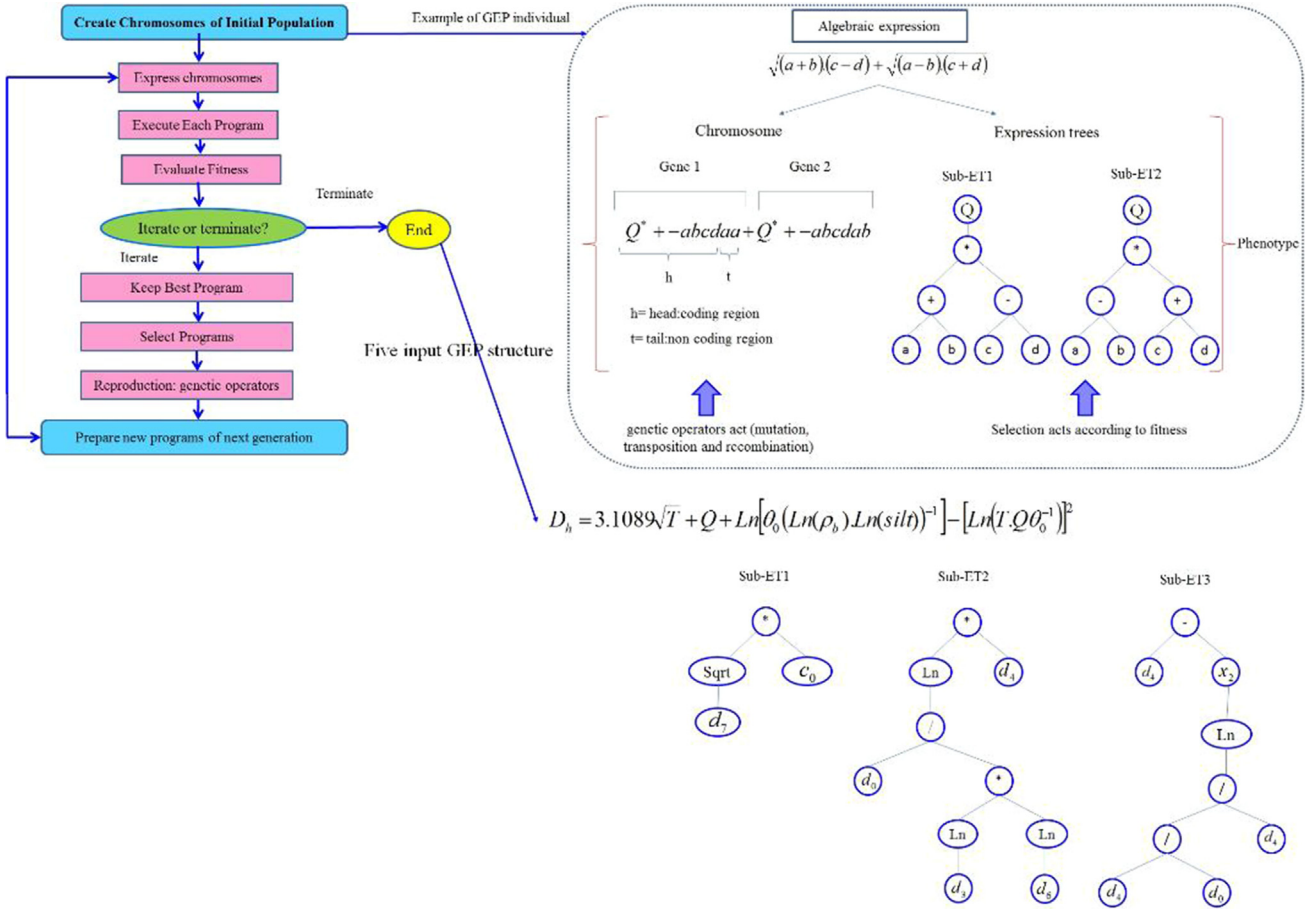

Fig. 4. Schematic representation of the employed GEP.

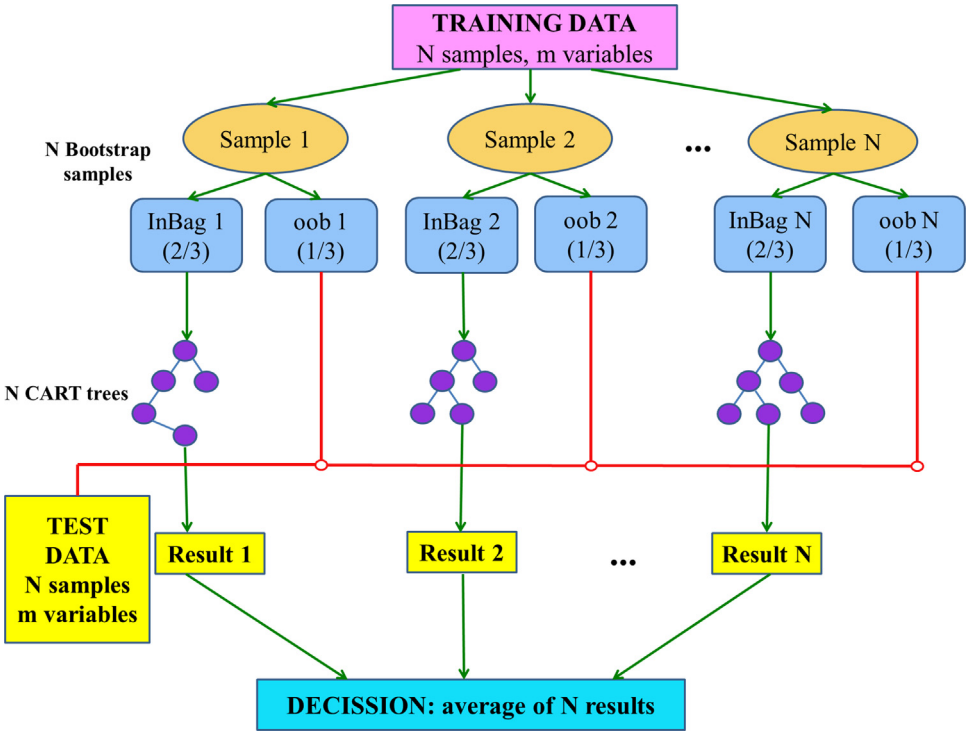

Fig. 5. A schematic view of the RF flowchart.

2.5. Study protocol

A major task with application of data driven approaches is selecting the appropriate input parameters that can easily simulate the target parameter's values. There are different input selection methods, from which, analysis of the physical aspects of the studied phenomenon might be a good candidate for selecting the inputs. Here, both the physical behavior of the studied phenomenon and the reports given by the published literature were considered for selecting the proper input variables. Hence, the emitter discharges (Q), soil texture factors (silt, sand and clay percentages), soil bulk density (ρ_b), saturated hydraulic conductivity (K_S) and the elapsed time (T) were considered as inputs for simulating the wetting front dimensions in all treatments (e.g. Al-Ogaidi et al., 2016). An additional emitter depth (D) variable was also considered in subsurface irrigation systems; while the ratio of irrigation cycle time to the total time of the irrigation process (T_{irr}/T_t) was considered in pulse irrigation mode.

Another major step with applying data driven models is partitioning the available patterns for training and testing the applied models. A common procedure would be partitioning the available data into two blocks, namely, training and testing data set. This division might be achieved randomly or by considering specific conditions of the studied phenomenon. Thus, the established model using the training data will be tested by a single data set (testing patterns). Although this is a straightforward procedure for developing and assessing the applied models, the outcomes might be misleading because all the available patterns have not been participated in model development/testing. Hence, other robust scanning procedures should be adopted for assessing the models' performances (e.g. Marti et al., 2013). In the present research, the powerful k-fold testing data scanning tool was adopted for all the studied experiments. So, all available patterns of each experiment (based on irrigation type/application mode) were divided into "k" blocks and the models were trained each time by using "k-1" blocks, and then tested using the patterns of the remaining one block. The process was repeated until all available patterns of each experiment were incorporated in both the training and testing stages. The values of "k" might be defined based on different criteria. Here, different criteria were used to define the "k" values of k-fold testing (i.e. defining the test subset) per experiment, e.g. soil type-based/emitter depth-based and T_{irr}/T_t-based partitioning of data. Table 2 provides general information on the available patterns of each irrigation type/application mode. Based on the information presented in this table, for the surface irrigation system with continuous application mode, the patterns were divided based on soil type (k = 6). In the pulse mode, two criteria were used: the soil type (k = 3) and the ratio of irrigation cycle time to the total time of the irrigation process (T_{irr}/T_t) (k = 3). So, 12 training testing procedures were carried out per model for each simulated parameter and a total of 48 procedures conduced in surface irrigation type [for GEP and RF models in simulating wetting diameter (D_h) and depth (D_V)].

Attending to the subsurface irrigation system, the soil type (k = 6) and the emitter depth (k = 3) were used for dividing the available patterns in continuous application. A number of 9 train-test procedures were done per model per simulated parameter [D_h, D_V and upward water movement (Z_{up})], so totally 54 processes were fulfilled here. Further, the soil type (k = 3), the emitter depth (k = 2) and the T_{irr}/T_t ratio (k = 3) were used for partitioning the blocks and defining the k values for subsurface-pulse irrigation. 48 training–testing procedures were carried out in this case. Fig. 6 presents a schematic view of the irrigation types/application modes along with the corresponded defined k-fold test scenarios.

2.6. Evaluation criteria

Four statistical evaluation indices were used for assessing the adopted methodology, namely, the coefficient of determination (r^2), the root mean square error ($RMSE$), the scatter index (SI) and the Nash-Sutcliffe coefficient (NS) as follows:

$$r^2 = \left[\frac{\sum_{i=1}^{n} (x_i^{target} - \bar{x}^{target})(x_i^{mod\ el} - \bar{x}^{mod\ el})}{\sqrt{\sum_{i=1}^{n} (x_i^{target} - \bar{x}^{target})^2 \sum_{i=1}^{n} (x_i^{mod\ el} - \bar{x}^{mod\ el})^2}} \right]^2 \quad (10)$$

$$RMSE = \sqrt{\frac{1}{n} \sum_{i=1}^{n} (x_i^{mod\ el} - x_i^{target})^2} \quad (11)$$

$$SI = \frac{RMSE}{\bar{x}^{target}} = \frac{\sqrt{\frac{1}{n} \sum_{i=1}^{n} (x_i^{mod\ el} - x_i^{target})^2}}{\bar{x}^{target}} \quad (12)$$

$$NS = 1 - \frac{\sum_{i=1}^{n} (x_i^{mod\ el} - x_i^{target})^2}{\sum_{i=1}^{n} (x_i^{target} - \bar{x}^{target})^2} \quad (13)$$

In these equations, $x^{mod\ el}$ and x^{target} stand for the simulated and target values at the i^{th} time step, respectively. $\bar{x}^{mod\ el}$ and $\bar{x}^{target}$ are the corresponding mean values of the simulated parameter, respectively. n denotes number of patterns. The perfect value of r^2 is unity representing a similar trend between the observed and simulated values. As this index is sensitive to outliers, it shouldn't be used alone as a model assessment tool (Legates and McCabe, 1999). $RMSE$ measures the weighted distances between the simulated and observed values through assigning more weights to the larger error magnitudes. Moreover, its weighted version, i.e. SI is an appropriate tool for comparative evaluation of the models/treatments because it eliminates the impact of the observed values' magnitude from $RMSE$ and can provide clear insight about the models performance. Finally, the NS coefficient that compares the variance ratios can vary between $-\infty$ and 1 (perfect

Table 2
General information on the available patterns and applied soft computing methods.

Irrigation Type	Application mode	Soil types No.	Emitter depth No.	T_{irr}/T_t No.	Available patterns for D_h	Available patterns for D_V	Available patterns for Z_{up}
Surface	Continuous	6	–	–	205	225	–
	Pulse	3	–	3	406	557	–
Subsurface	Continuous	6	3	–	528	575	489
	Pulse	3	2	3	885	825	1374

Note: D_h: wetting radius, D_V: wetting depth, Z_{up}: upward water movement in subsurface irrigation system (see Fig. 1).

Overview of the characteristics of the applied soft computing methods (Shiri et al., 2020)

Method	Learning algorithm	General category of the base model	General category of the learning algorithm
GEP	Basic fitness function based on the error or residual	Evolutionary computation	Root relative square error
RF	Ensemble learning	Machine learning Bootstrap aggregating	Machine learning Bootstrap aggregating

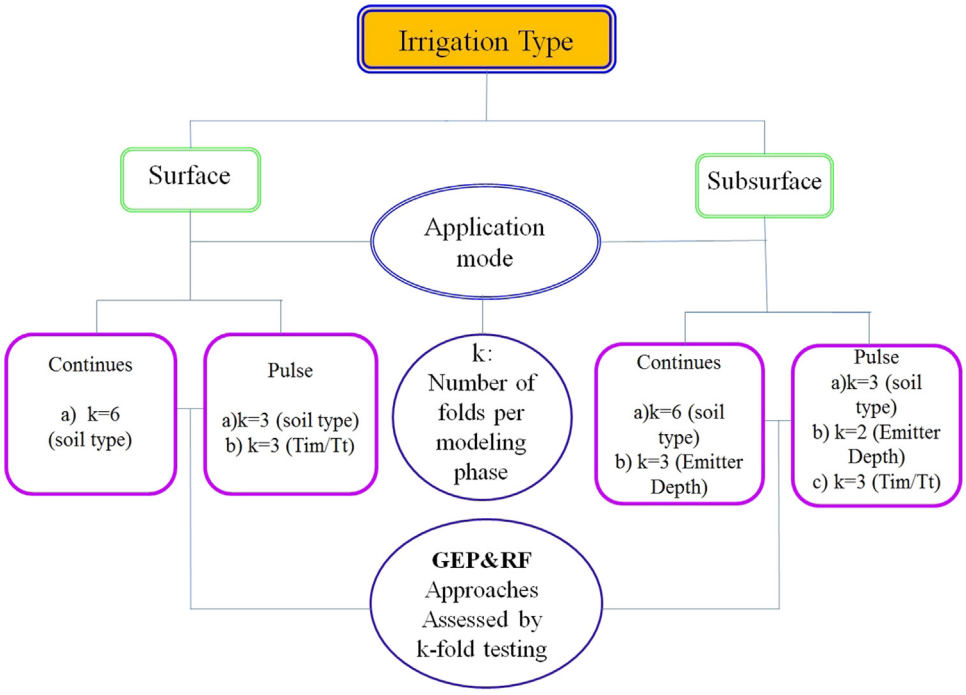

Fig. 6. Representation of the study flowchart and defining "k" values of k-fold testing.

Table 3
Global statistical indices of the GEP and RF models.

Irrigation type	Application mode		GEP					RF				
			r^2	*RMSE*	*SI*	*NS*	*CRM*	r^2	*RMSE*	*SI*	*NS*	*CRM*
Surface	Continuous	$D_{h\text{-}a}$	0.888	6.032	0.142	0.887	−0.008	0.854	8.621	0.203	0.770	0.006
		$D_{V\text{-}a}$	0.921	3.047	0.159	0.921	0.001	0.872	5.135	0.268	0.778	0.042
	Pulse	$D_{h\text{-}a}$	0.981	1.068	0.044	0.981	−0.003	0.948	6.824	0.135	0.802	−0.004
		$D_{h\text{-}b}$	0.919	2.169	0.125	0.911	−0.009	0.911	6.925	0.137	0.800	−0.009
		$D_{V\text{-}a}$	0.989	1.212	0.045	0.989	0.135	0.931	4.089	0.153	0.877	−0.001
		$D_{V\text{-}b}$	0.980	1.625	0.060	0.954	−0.137	0.921	4.218	0.157	0.869	0.007
Subsurface	Continuous	$D_{h\text{-}a}$	0.946	6.666	0.199	0.865	−0.074	0.939	5.001	0.149	0.897	0.004
		$D_{h\text{-}b}$	0.939	4.070	0.121	0.932	0.006	0.937	5.010	0.145	0.898	0.004
		$D_{V\text{-}a}$	0.922	6.051	0.333	0.780	0.234	0.911	8.072	0.485	0.568	0.012
		$D_{V\text{-}b}$	0.877	3.890	0.235	0.884	−0.001	0.912	4.568	0.240	0.812	−0.004
		$Z_{up\text{-}a}$	0.820	3.030	0.316	0.416	0.001	0.828	3.125	0.328	0.456	0.003
		$Z_{up\text{-}b}$	0.802	2.865	0.238	0.522	−0.114	0.811	2.900	0.241	0.520	−0.004
	Pulse	$D_{h\text{-}a}$	0.976	3.805	0.096	0.926	−0.014	0.945	5.397	0.134	0.855	0.001
		$D_{h\text{-}b}$	0.968	2.772	0.070	0.957	−0.006	0.948	4.321	0.108	0.950	0.003
		$D_{h\text{-}c}$	0.965	3.754	0.094	0.929	0.041	0.946	4.631	0.115	0.893	0.001
		$D_{V\text{-}a}$	0.921	3.718	0.198	0.831	0.013	0.911	3.800	0.200	0.825	0.003
		$D_{V\text{-}b}$	0.863	4.122	0.224	0.737	0.106	0.921	6.135	0.330	0.876	0.001
		$D_{V\text{-}c}$	0.905	6.955	0.383	0.618	−0.339	0.900	7.010	0.383	0.600	0.003
		$Z_{up\text{-}a}$	0.916	1.428	0.124	0.808	−0.032	0.910	1.500	0.130	0.795	0.001
		$Z_{up\text{-}b}$	0.853	1.352	0.118	0.828	0.003	0.850	1.430	0.124	0.800	0.004
		$Z_{up\text{-}c}$	0.864	1.886	0.165	0.672	−0.072	0.821	1.900	0.170	0.654	−0.001
		Traditional methods										
		Schwartzman						Kandelous				
Surface continuous irrigation		D_h	0.830	15.450	0.418	−0.353	−0.360	–	–	–	–	–
		D_V	0.890	6.200	0.288	0.684	0.210	–	–	–	–	–
Sub–surface continuous irrigation		D_h	–	–	–	–	–	0.940	7.500	0.225	0.696	0.144
		D_V	–	–	–	–	–	0.640	10.704	0.548	−0.143	0.430
		Z_{up}	–	–	–	–	–	0.880	2.003	0.185	0.712	−0.013

Note: Note: a, b and c suffixes have been introduced in Fig. 6. Underlined values corresponded to the best models of each category. *RMSE* is in cm.

performance of the model).

The applied indices were computed for all testing subsets (defined through k-fold testing) and the complete data set. In computing the indices for the complete data set, a global matrix was built comprising all simulated-observed patters of each testing sub-set and then, the statistical performance indices were derived using all available patterns.

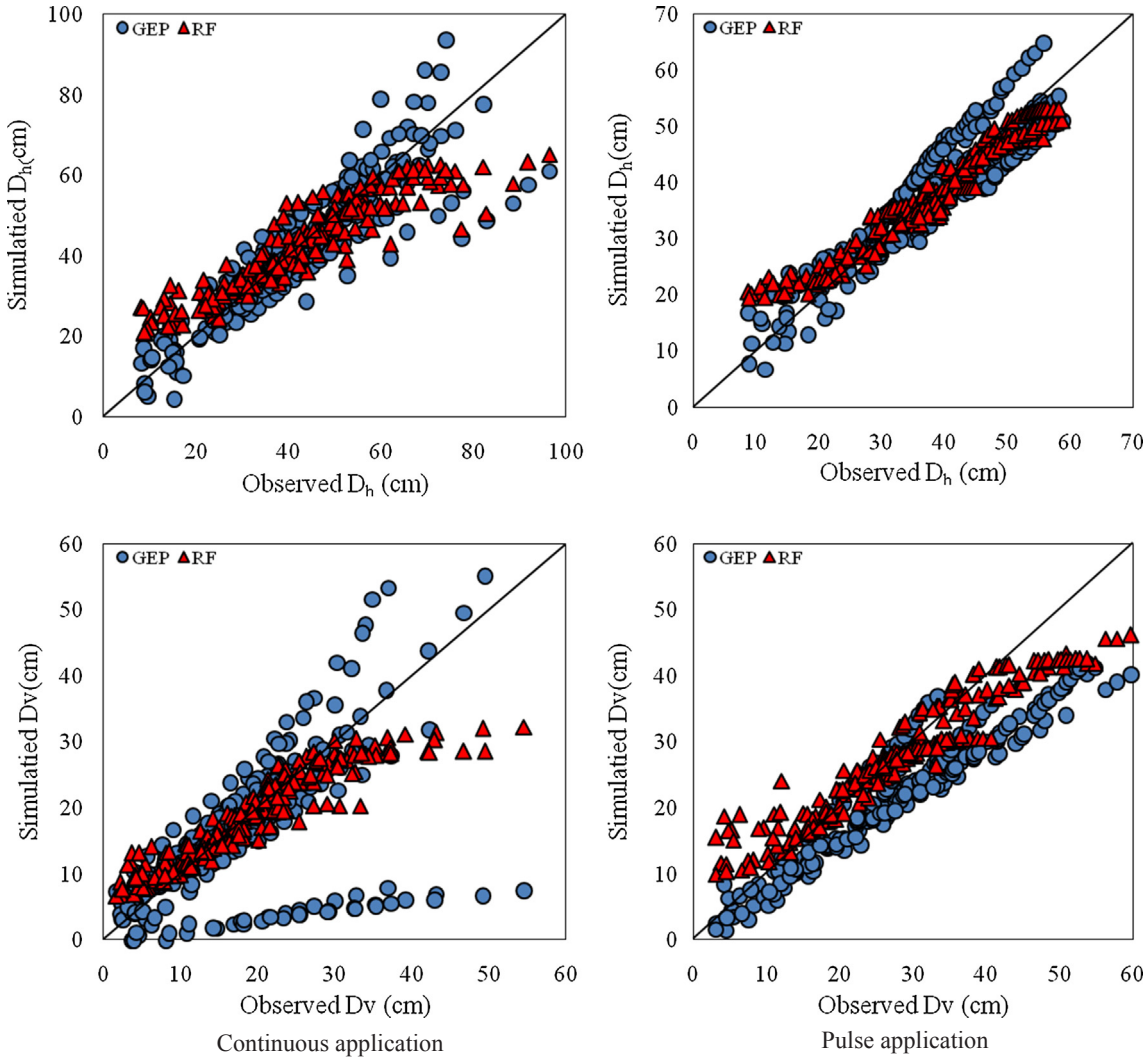

Fig. 7. Observed vs. simulated values of the D_h and D_V for surface drip irrigation system.

3. Results and discussions

Table 3 presents the global statistical indices of the GEP and RF models for all the studied treatments. The reported values correspond to the complete data set that have been computed by using observed-simulated sets of all k-fold testing stages outcomes. As mentioned, different criteria were considered for partitioning the available patterns into training and testing subsets. The best models of each simulated parameter have been underlined to facilitate the comparative assessment of the models.

Attending to the surface irrigation experiments, it is clear from the table that the models gave more accurate results for pulse irrigation application than the continuous application for modeling both wetting diameter and depth (D_h and D_V, respectively) parameters. Differences between the *SI* and *NS* (ΔSI and ΔNS) values of the best models of the continuous and pulse applications were, respectively, 0.098 and 0.094 (GEP); and 0.068 and 0.032 (RF) for D_h. Similarly, the ΔSI and ΔNS values were 0.114 and 0.068 (GEP); and 0.115 and 0.099 (RF) for D_V. Comparing the performance accuracy of the models for continuous application (surface irrigation) revealed that D_h estimation models gave slightly better results than those of the D_V estimation models, while D_h and D_V estimation models presented similar performance accuracy in case of surface pulse irrigation. From the data division viewpoint (k definition criteria in k-fold testing; see Fig. 6), it can be clearly seen that using soil types for defining the test stages have produced more accurate results than using T_{irr}/T_t criterion. This might be linked to the characteristics of the moisture front movement in irrigation systems, where, a portion of front movement in pulse irrigation applications occurs at the systems' rest (off) time. This type of movement occurs when the discharge rate of the emitters are high, so the soil doesn't have enough capacity to deliver the irrigation water during the irrigation process (during the "on" time). Hence, given that the water is freely distributed in surface irrigation systems, and only a little part of movement occurs at rest time, the influence of soil type would be more than the T_{irr}/T_t ratio in this case. Finally, comparing the GEP and RF results with those of the Schwartzman model revealed that both the GEP and RF models presented more accurate results in surface continuous irrigation. The poor performance of the Schwartzman model might be linked to the experimental conditions under which, it has been developed (e.g. two emitter discharges as $1.1*10^{-6}$ and $5.6*10^{-6}$ m^3/s).

In case of the subsurface irrigation system, similar trends might be detected, where the models gave the most accurate results for pulse application with ΔSI and ΔNS magnitudes (for best models of the pulse and continuous applications) of 0.051 and 0.025 (GEP) and 0.037 and 0.052 (RF) in D_h estimations. In continuous application treatment, the models gave the best results for D_h simulation, followed by D_V and upward movement (Z_{up}). Using the emitter installation depth has produced better results than using soil type as data division criterion for continuous subsurface irrigation. Generally, the dimensions of the

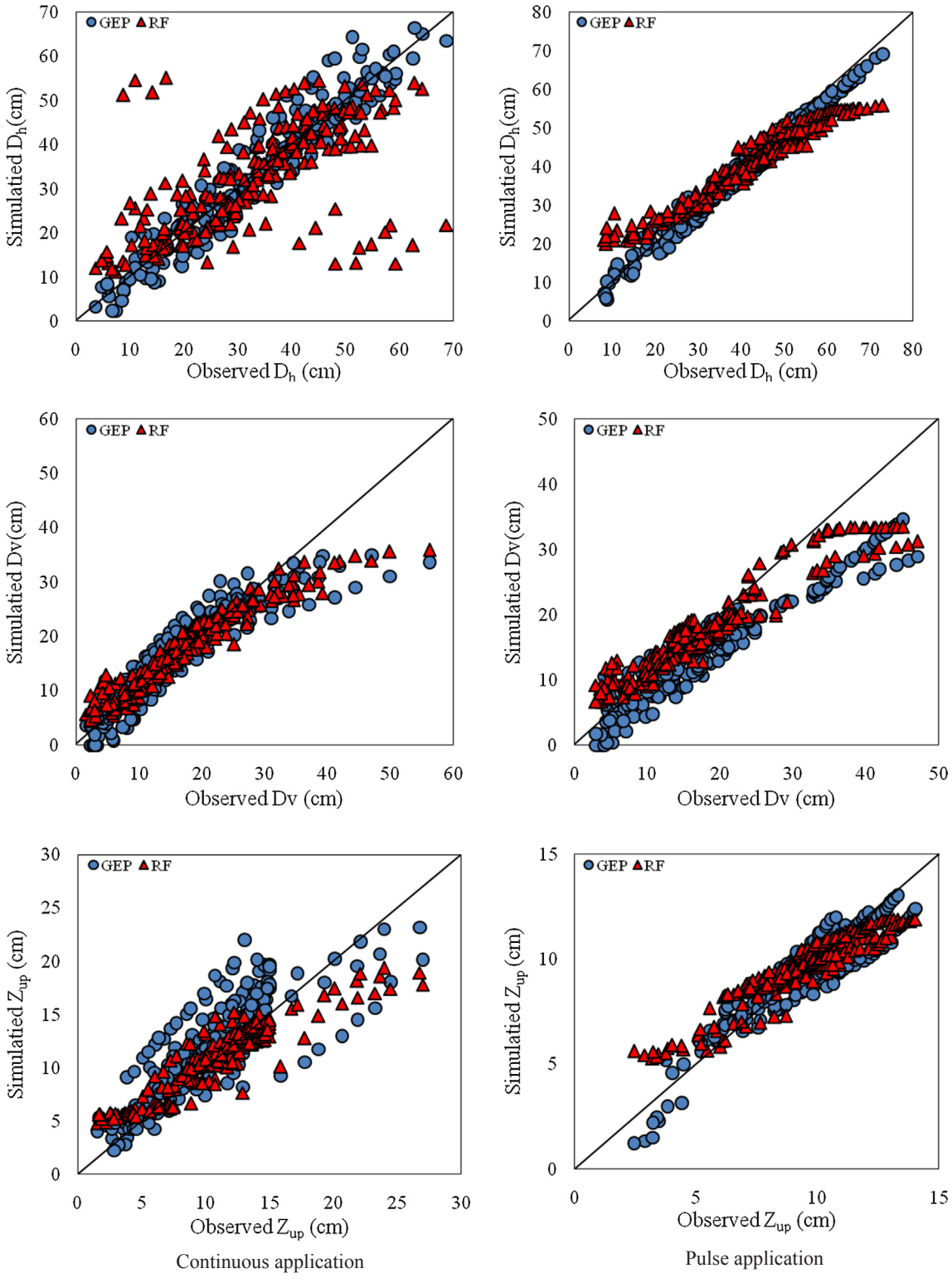

Fig. 8. Observed vs. simulated values of D_h, D_V and Z_{up} for the subsurface drip irrigation system.

wetted bulb of subsurface irrigation systems are influenced by the depths of subsurface emitter as well as the soil load over the emitter. This might explain the higher impact of emitter installation depth on modeling wetting front dimensions, which is in agreement with the conclusions obtained by Kandelous et al. (2008) and Singh et al. (2006). For subsurface pulse irrigation, the best outcomes belonged to D_h estimations followed by Z_{up} and D_V, respectively. Among the target parameters, the best estimations for D_h and Z_{up} were belonged to the models assessed by emitter depth variations, while the soil type-based partitioning the patterns gave the best results for D_V. Comparing these results with those of the Kandelous model for sub-surface continuous irrigation, it is seen that GEP and RF outperformed this model in estimating D_h and D_V, while the best results of Z_{up} estimation belonged to Kandelous model.

Figs. 7 and 8 display the global observed and simulated values of the target parameters for both the surface and subsurface drip irrigation

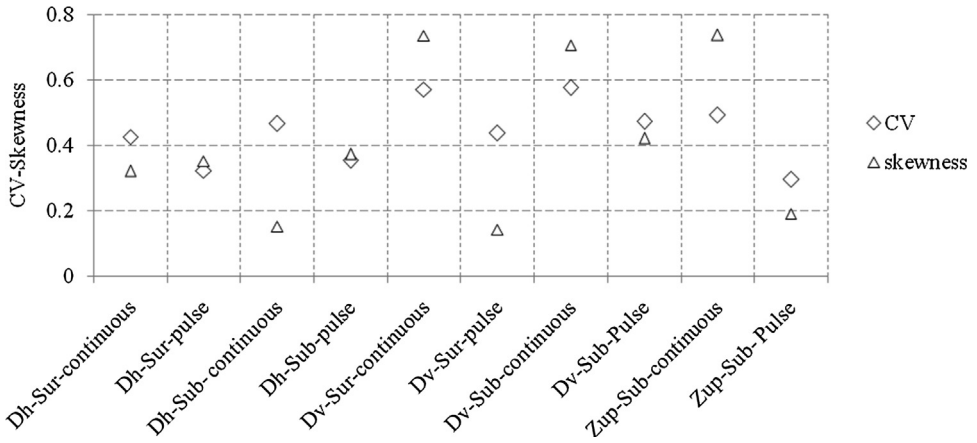

Fig. 9. Skewness coefficient and CV values of the studied variables.

Table 4
Summary of "*t*-test" and "*F*-test" statistics of the best models in simulating wetting front dimensions.

		GEP				RF			
		t	*t*-critical	*F*	*F*-critical	*t*	*t*-critical	*F*	*F*-critical
Surface irrigation									
Continuous	D_h	−0.797	1.971	1.089	1.260	0.435	1.971	2.479	1.260
	D_V	0.065	1.970	1.091	1.247	**2.279**	**1.970**	**2.468**	**1.247**
Pulse	D_h	1.260	1.965	1.047	1.178	−1.484	1.967	**1.842**	**1.203**
	D_V	0.778	1.964	**0.968**	**0.869**	−0.146	1.964	**1.860**	**1.149**
Subsurface irrigation									
Continuous	D_h	−1.44	1.964	1.017	1.154	0.637	1.964	1.079	1.154
	D_V	−4.166	1.964	1.131	1.147	1.464	1.964	1.139	1.147
	Z_{up}	0.991	1.964	1.330	1.160	0.344	1.964	1.998	1.160
Pulse	D_h	−1.188	1.962	1.042	1.117	0.182	1.962	2.213	1.117
	D_V	**3.316**	**1.962**	1.016	1.121	0.464	1.962	1.682	1.121
	Z_{up}	−0.520	1.962	**1.577**	**1.092**	0.400	1.962	**1.706**	**1.092**

Note: Highlighted values show the significant difference at 0.05 significance level. The rest of the cases are non-significant differences at the same level.

Table 5
Computational characteristics of the applied soft computing models per studied case.

Irrigation type	Application mode		GEP			RF		
			Computational cost	Run time (s)	Convergence speed	Computational cost	Run time (s)	Convergence speed
Surface	Continuous	$D_{h\text{-}a}$	5911	58	102	138	2	59
		$D_{V\text{-}a}$	4375	54	81	132	3	44
	Pulse	$D_{h\text{-}a}$	10,007	178	56	158	2	79
		$D_{h\text{-}b}$	8577	151	57	148	4	37
		$D_{V\text{-}a}$	10,278	210	49	180	10	18
		$D_{V\text{-}b}$	10,248	232	44	136	3	42
Subsurface	Continuous	$D_{h\text{-}a}$	4638	92	50	800	18	44
		$D_{h\text{-}b}$	8157	135	60	816	12	68
		$D_{V\text{-}a}$	5461	109	50	900	11	81
		$D_{V\text{-}b}$	2418	40	60	855	11	81
		$Z_{up\text{-}a}$	10,811	223	48	1000	12	83
		$Z_{up\text{-}b}$	10,875	199	54	1170	14	84
	Pulse	$D_{h\text{-}a}$	4631	140	33	340	4	85
		$D_{h\text{-}b}$	5699	132	43	440	4	110
		$D_{h\text{-}c}$	5904	167	35	269	7	38
		$D_{V\text{-}a}$	5155	134	38	269	13	21
		$D_{V\text{-}b}$	7640	138	55	347	18	19
		$D_{V\text{-}c}$	6750	188	36	347	22	16
		$Z_{up\text{-}a}$	6299	226	28	190	6	31
		$Z_{up\text{-}b}$	4356	155	28	290	18	16
		$Z_{up\text{-}c}$	7810	286	27	390	30	13

Note: a, b and c suffixes have been introduced in Fig. 6. Computational cost in GEP and RF methods are, respectively, the generations' number and tree numbers. Convergence speed equals computational cost divided by runtime.

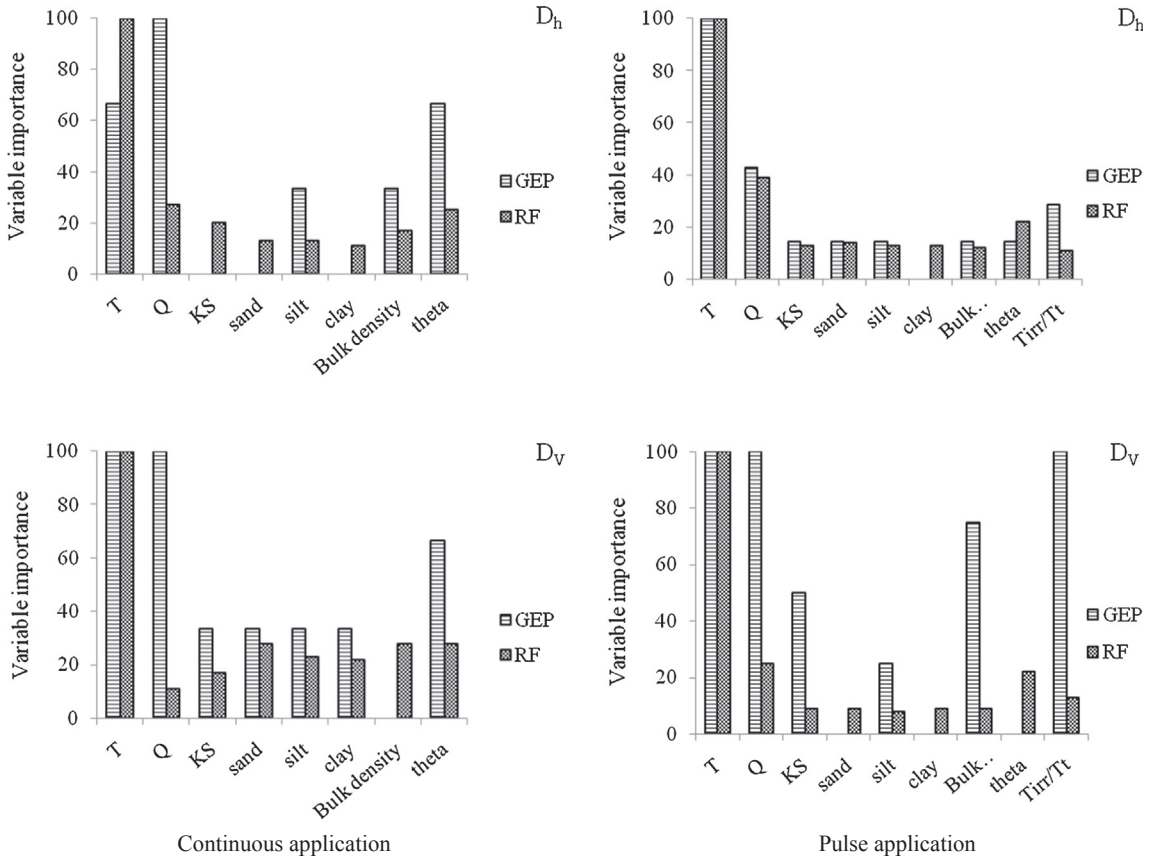

Fig. 10. Importance of each input parameter given by the applied models-Surface drip irrigation.

experiments, respectively. These values have been obtained through pooling the individual observed-simulated values of each model per test (k-fold) stage (as defined before). There are good matches between the target and simulated values in all cases, although some scatters (underestimations) from the identity function (1:1 line) can be clearly observed in some cases. More specifically, the observed and simulated values of D_h showed obvious scatters for surface drip irrigation with continuous application mode. Similar scatters are also clear for Zup estimation of subsurface pulse irrigation. Most of the underestimations shown in the figures corresponded to D_V estimations, especially for continuous applications. Obvious scatters are also observed for Z_{up} estimation in subsurface continuous application. These specific observations are confirmed through analyzing the *SI* values of Table 3. This might be linked to the skewness and coefficient of variation (CV) values of D_V and Z_{up} as can be seen in Fig. 9. From the figure it is clear that the values of these indices are higher than the others that can make their simulations difficult.

Furthermore, the performances of the best models were assessed through statistical tests. So, the null hypothesis of equal mean and variance at 0.05 significance level was considered and tested using the "*t*-test" and "*F*-test", respectively. Table 4 presents the "*t*" and "*F*" values as well as their critical thresholds for the studied models. From the table it is clear that in most of the cases the null hypothesis is true and differences between the mean and variance of the observed and simulated values are non-significant. However, significant differences between the mean and variance values are observed as highlighted in Table 4. Attending to D_V simulation in surface continuous irrigation, both the tests showed significant differences between observed-simulated pairs by using RF method. Using the RF, significant differences of variances were confirmed in modeling both D_h and D_V in surface pulse irrigation, where GEP shows a similar difference for modeling D_V, too. Finally, significant differences of variance can be observed for Z_{up} modeling in sub-surface pulse irrigation. So, it is clear that, with minor exception, GEP has showed a good ability for modeling wetting front dimensions.

Table 5 summarizes some metrics of the computational cost for the GEP and RF models in the studied treatments. Figs. 10 and 11 shows the importance of each input variable for the studied cases (optimal models) given by both the GEP and RF models. In case of the surface irrigation experiments, the maximum weight was given for the elapsed time (*T*) by the GEP and RF model in both continuous and pulse applications, except for D_h (continuous application) where GEP assigned the maximum weight to flow discharge (*Q*). Further, D_V estimation GEP models gave the similar weights (highest values) for *T* and *Q* parameters in continuous application and for *T*, *Q* and T_{irr}/T_t in pulse application modes. For the subsurface irrigation experiments, *T*, *Q* and T_{irr}/T_t variables have had the highest impact on D_h and D_V modeling, while soil bulk density and initial moisture content have presented higher influence on modeling Z_{up} for both the continuous and pulse applications.

Attending to the other input variables, differences/similarities might be detected between the GEP and RF models in all cases. Moreover, the figures clearly show that GEP has not selected some input variables for modeling the target parameters. A first reason for such discrepancies might be the applied models' theorem. GEP develops the constants and structure of the obtained formulae, simultaneously, so that the case-specified constants are included in the formulation of the studied phenomenon. Nevertheless, for reduction of the obtained genetic tress size, the parsimony pressure was employed. On the other hand, RF is a tree-based group method, where all trees are dependent of a collection of random variables, and the forest is grown from many regression trees put together and from a group. Another reason for differences between the input selections in the studied cases might be the physical facts of the simulated parameters. In spite of the all

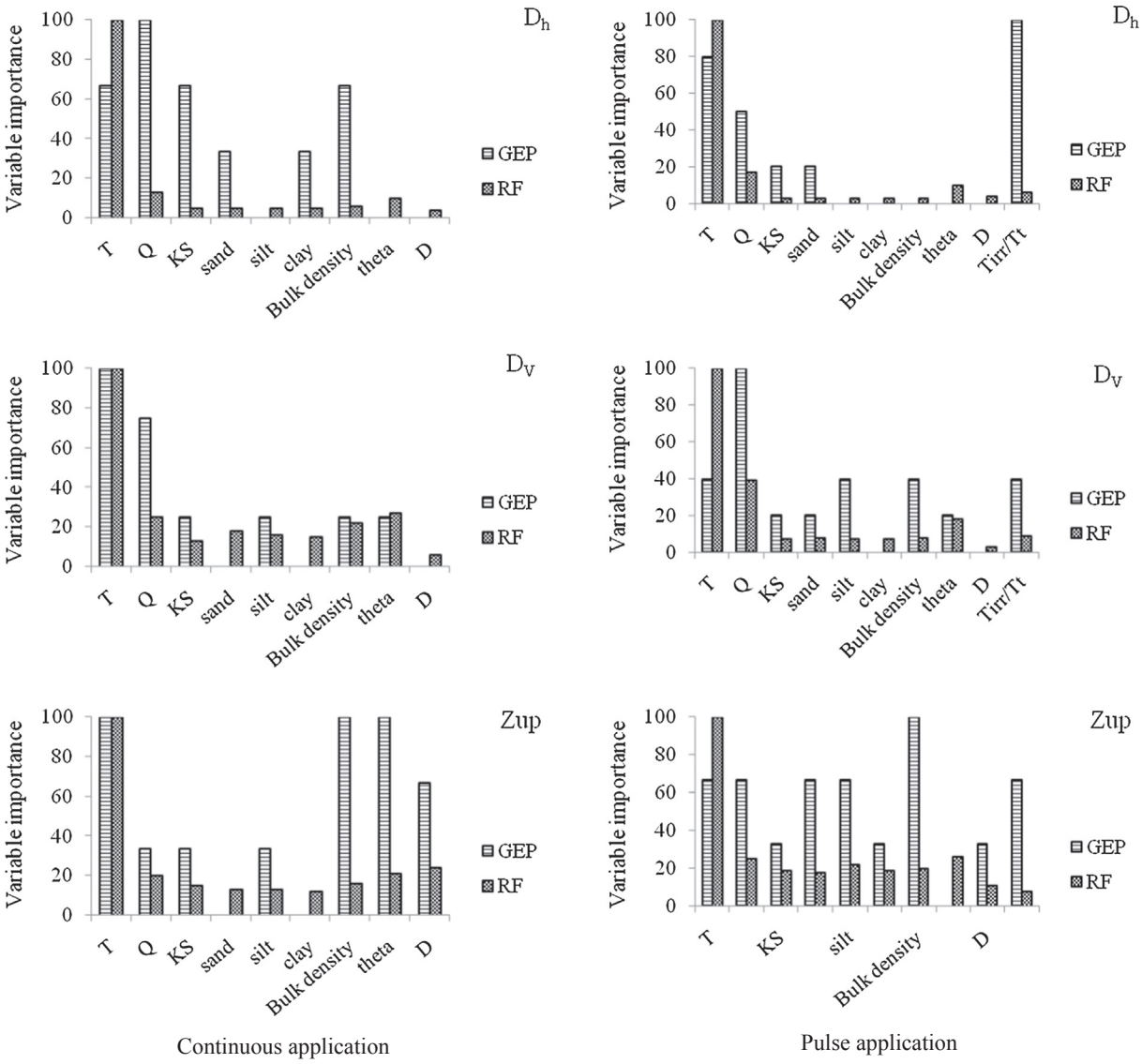

Fig. 11. Importance of each input parameter given by the applied models-Subsurface drip irrigation.

similarities/differences between the input selections of the GEP and RF models, it is evident that RF has utilized all introduced input variables for simulating the target parameters (even by giving lower weights), while GEP has picked up some inputs (based on the studied parameter) and simulated the target values with higher accuracy. Hence, it might be concluded that GEP can handle these kinds of simulations by using limited input variables. This is of special importance especially when the available data are limited to some easily measured parameters and one seek to get acceptable results of simulations using those limited variables.

Further, the effect of some variables on wetting front dimensions was analyzed. First, the results showed that the with increasing the elapsed time and the emitter flow discharge, the observed and simulated values of D_h, D_V and Z_{up} were increased for all treatments. This might be anticipated because with increasing the elapsed time/flow discharge the volume of water being delivered into soil profile will be increased. Nonetheless, the dimensions of wetting front were influenced by the emitter depth in subsurface irrigation system, where the larger the emitter depth, the higher the observed and simulated D_V and Z_{up} values. This partial conclusion is in good agreement with the results reported by Singh et al. (2006).

Summarizing, it was seen that both the models can produce acceptable results in simulating wetting front dimensions in the soil media, although some monotonous fluctuations in the degree of performance accuracy can be observed as demonstrated in the tables and figures. Despite their good degree of accuracy, the models developed would have some limitations such as their validity in the range of the data introduced to the models. On the other hand, the robust k-fold testing procedure was adopted with different strategies to increase the generalizability of the applied models. So, it might be concluded that the models can be used for the similar irrigation systems with various soil type, system, discharge and emitter characteristics subjected to a quantitative limitation of the input variables to the range of those utilized here. Further studies might be conducted using more soil types, emitter depths and discharge variations to reinforce these conclusions.

4. Conclusions

Modeling wetting front dimensions, e.g. diameter, depth and upward movement (D_h, D_V and Z_{up}, respectively) through GEP and RF models (assessed by k-fold testing) were reported in the present research. The experiment were conducted for surface and sub-surface drip irrigation systems with continuous and pulse water applications. Different soil (e.g. particles percentage, bulk density, initial moisture

content and saturated hydraulic conductivity) and system (e.g. emitter flow discharge, irrigation duration (elapsed time), emitter installation depth and T_{irr}/T_t) parameters were used as input variables to feed the employed models. The obtained results of the present research revealed that:

1. For both the surface/sub-surface irrigation systems, the pulse application mode presented more accurate results than the continuous application.
2. In all the treatments, wetting diameter (Dh) simulation gave better results than the D_V and Z_{up} estimation.
3. Using soil type as a criterion for defining the data partitioning mode in k-fold testing process was the best choice in surface irrigation system. For the subsurface system, the best criterion for defining "k" values was emitter installation depth.
4. The models showed underestimation trend for higher D_h and D_V values.

CRediT authorship contribution statement

Jalal Shiri: Conceptualization, Methodology, Writing - original draft. **Bakhtiar Karimi:** Conceptualization, Data curation, Methodology. **Nazir Karimi:** Experiment conducting. **Mohammad Hossein Kazemi:** Modeling. **Sepideh Karimi:** Modeling, Writing - review & editing.

Declaration of Competing Interest

The authors declare that they have no known competing financial interests or personal relationships that could have appeared to influence the work reported in this paper.

References

Al-Ghobari, H.M., El-Marazky, M.S., Dewidar, A.Z., Mattar, M.A., 2018. Prediction of wind drift and evaporation losses from sprinkler irrigation using neural network and multiple regression techniques. Agric. Water Manage. 195, 211–221.

Al-Ogaidi, A.A.M., Wayayok, A., Rowshona, M.K., Abdullah, A.F., 2016. Wetting patterns estimation under drip irrigation systems using an enhanced empirical model. Agric. Water Manage. 176, 203–213.

Amin, M.S.M., Ekhmaj, A.I.M., 2006. DIPAC- drip irrigation water distribution pattern calculator. In: 7th Int Micro Irrigation Congress PWTC, Kuala Lumpur, Malaysia, pp. 503–513.

Arbat, G., Puig-Bargués, J., Duran-Ros, M., Barragán, J., Ramírez de Cartagena, F., 2013. Drip-Irriwater: computer software to simulate soil wetting patterns under surface drip irrigation. Comput. Electron. Agric. 98, 183–192.

Breiman, L., 2001. Random Forests. Machine Learning 45 (1), 5–32.

Cook, F.J., Thorburn, P.J., Fitch, P., Bristow, K.L., 2003. WetUp: a software tool to display approximate wetting patterns from drippers. Irrig. Sci. 22, 129–134.

Ekhmaj, A.I., Abdulaziz, A.M., Almdny, A.M., 2007. Artificial neural networks approach to estimate wetting pattern under point source trickle irrigation. African Crop Science Conference, pp. 1625–1630.

Elmaloglou, S., Diamantopoulos, E., 2009. Effects of hysteresis on redistribution of soil moisture and deep percolation at continuous and pulse drip irrigation. Agric. Water Manag. 96, 533–538.

Elmaloglou, S., Soulis, K.X., Dercas, N., 2013. Simulation of soil water dynamics under surface drip irrigation from equidistant line sources. Water Resour. Manag. 27, 4131–4148.

Ferreira, C., 2001. Gene expression programming: a new adaptive algorithm forsolving problems. Complex Syst. 13 (2), 87–129.

Ferreira, C., 2006. Gene Expression Programming: Mathematical Modeling by anArtificial Intelligence. Springer, Berling, Heidelberg New York, pp. 478.

Golestani Kermani, S., Sayari, S., Kisi, O., Zounemat-Kermani, M., 2019. Comparing data driven models versus numerical models in simulation of waterfront advance in furrow irrigation. Irrig. Sci. 37 (5), 547–560.

Hammami, M., Zayani, K., 2016. An analytical approach to predict the moistened bulb volume beneath a surface point source. Agric. Water Manag. 166, 123–129.

Hastie, T., Tibshirani, R., Friedman, J., 2009. The Elements of Statistical Learnin. Springer, New York.

Hinnell, A.C., Lazarovitch, N., Furman, A., Poulton, M., Warrick, A.W., 2010. Neuro-Drip: estimation of subsurface wetting patterns for drip irrigation using neural networks. Irrig. Sci. 28, 535–544.

Kandelous, M.M., Liaghat, A., Abbasi, F., 2008. Estimation of soil moisture pattern in subsurface drip irrigation using dimensional analysis method. J. Agri. Sci. 39 (2), 371–378 (in Persian).

Kandelous, M.M., Simunek, J., 2010a. Comparison of numerical, analytical and empirical models to estimate wetting pattern for surface and subsurface drip irrigation. Irrig. Sci. https://doi.org/10.1007/s00271-009-0205-9.

Kandelous, M.M., Simunek, J., 2010b. Numerical simulations of water movement in a subsurface drip irrigation system under field and laboratory conditions using HYDRUS-2D. Agric. Water Manag. 97 (2010), 1070–1076.

Kandelous, M.M., Simunek, J., Van Genuchten, M.T.H., Malek, K., 2011. Soil water content distributions between two emitters of a subsurface drip irrigation system. Soil Phys. 75 (2), 488–497.

Karimi, B., Mirzaei, F., Sohrabi, T., 2015. Developing equations to estimate wetted area pattern for surface and subsurface drip irrigation systems by dimensional analysis. Iran. J. Water Soil Sci. 25 (3), 241–252.

Karimi, B., Mohammadi, P., 2018. Evaluation of artificial neural network for estimating the advance velocity of the wetting front in drip irrigation. Iran. J. Water Res. Agric. 32 (1), 79–92.

Karmeli, D., Peri, G., 1974. Basic principles of pulse irrigation. Irrigat. Drainage Divis. 100 (3), 309–319.

Khanmohammadi, N., Besharat, S., 2018. Wetting pattern dimensions determination in drip irrigation by coupling the HYDRUS-2D software and backingham π theorem in texturally different soils. Iran. J. Appl. soil Res. 6 (2), 109–118.

Khattak, M.Sh., Ali, W., Ajmal, M., Khalil, T.M., Ahmad, J., Malik, A., Akbar, Gh., 2017. Assessment of wetted irrigation patterns for inline and online emitters in different soil textures. Himalayan Earth Sci. 50 (2), 149–163.

Koza, J.R., 1994. Genetic programming as a means for programming computers by natural selection. Stat. Comput. 4 (2), 87–112.

Landeras, G., Bekoe, E., Ampofo, J., Logah, F., Diop, M., Cisse, M., Shiri, J., 2018. New lternatives for reference evapotranspiration estimation in West Africa using limited weather data and ancillary data supply strategies. Theor. Appl. Climatol. 132, 701–716.

Lazarovitch, N., Poulton, M., Furman, A., Warrick, A.W., 2009. Water distribution under trickle irrigation predicted using artificial neural networks. J. Eng. Math. 64, 207–218.

Legates, D.R., McCabe, G.J., 1999. Evaluating the use of goodness-of-fit measures in hydrologic and hydroclimatic validation. Water Resour. Res. 35 (1), 233–241.

Liu, Zhigang, Xu, Qinchao, 2018. Wetting patterns estimation in cultivation substrates under drip irrigation. Desa. Water Treat. 112 (2018), 319–324.

Malek, K., Peters, R.T., 2011. Wetting pattern models for drip irrigation: new empirical model. J. Irrig. Drain. Eng. 137, 530–536.

Maroufpoor, S., Shiri, J., Maroufpoor, E., 2019. Modeling the sprinkler water distribution uniformity by data-driven methods based on effective variables. Agric. Water Manag. 215 (2019), 63–73.

Maroufpoor, E., Sanikhani, H., Emamgholizadeh, S., Kisi, O., 2018. Estimation of wind drift and evaporation losses from from sprinkler irrigation system by different data-driven methods. J. Irrig. Drain. 67 (2018), 222–232.

Marti, P., Shiri, J., Duran-Ros, M., Arbat, G., Cartagena, F.R., Puig-Bargues, J., 2013. Artificial neural networks vs. gene expressions programming for estimating outlet dissolved oxygen in micro irrigation sand filters fed with effluents. Comput. Electron. Agric. 99, 176–185.

Mohammadbeigi, A., Mirzaei, F., Ahraf, N., 2017. Simulation of soil moisture distribution under drip irrigation pulsed and continuous in dimensional analysis method. Iran. J. Water Soil Conserv. 23 (6), 163–180.

Mostaghimi, S., Mitchell, J.K., 1983. Pulsed trickling effect on soil moisture distribution. J. Water Resour. Bull. 19 (4), 605–612.

Najafzadeh, M., Shiri, J., Sadeghi, G., Ghaemi, A., 2018. Prediction of the friction factor in pipes using model tree. Ish. J. Hydraul. Eng. 24, 9–15.

Schaap, M.G., Leij, F.J., van Genuchten, M.T., 2001. Rosetta: a computer program for estimating soil hydraulic parameters with hierarchical pedotransfer functions. J. Hydrol. 251, 163–176.

Schwartzman, M., Zur, B., 1986. Emitter Spacing and Geometry of Wetted Soil Volume. J. Irrig. Drain Eng. 112 (3), 242–253.

Šejna, M., Simunek, J., van Genuchten, M.T., 2014. The HYDRUS software package for simulating two- and three-dimensional movement of water, heat, and multiple solutes in variably-saturated porous media, version 2.04 (PC Progress, Prague, Czech Republic).

Singh, D.K., Rajput, T.B.S., Sikarwar, H., Ahmad, V.T., 2006. Simulation of soil wetting pattern with subsurface drip irrigation from line source. Agric. Water Manag. 83, 130–134.

Shiri, J., Kim, S., Kisi, O., 2014. Estimation of daily dew point temperature using genetic programming and neural networks approaches. Nord. Hydrol. 45, 165–181.

Shiri, J., Keshavarzi, A., Kisi, O., Karimi, S., 2017a. Using soil easily measured parameters for estimating soil water capacity: soft computing approaches. Comput. Electron. Agric. 141, 327–339.

Shiri, J., Keshavarzi, A., Kisi, O., Karimi, S., Iturraran-Viveros, U., 2017b. Modeling soil bulk density through a complete data scanning procedure: heuristic alternatives. J. Hydrol. 549, 592–602.

Shiri, J., Zounemat-Kermani, M., Kisi, O., Mohsenzadeh Karimi, S., 2020. Comprehensive assessment of 12 soft computing approaches for modelling reference evapotranspiration in humid locations. Meteorol. Appl. https://doi.org/10.1002/met.1841.

Subbaiah, R., 2013. A review of models for predicting soil water dynamics during trickle irrigation. Irrig. Sci. 31, 225–258.